Distribution Agreement

Jiarui Yan April 10, 2023

Spectroscopic Studies of two f-Block Metal Compound

by

Jiarui Yan

Michael Heaven
Adviser

Chemistry

Michael Heaven

Adviser

James Kindt

Committee Member

Antonio Brathwaite

Committee Member

2023

Spectroscopic Studies of two f-Block Metal Compound

By

Jiarui Yan

Michael Heaven

Adviser

An abstract of
a thesis submitted to the Faculty of Emory College of Arts and Sciences
of Emory University in partial fulfillment
of the requirements of the degree of
Bachelor of Science with Honors

Chemistry

2023

Abstract

Spectroscopic Studies of two f-Block Metal Compound

By Jiarui Yan

Signal transmitted through the high-altitude atmosphere is fluctuated and scintillated because of the natural variation of electron density in the ionosphere. In trying to achieve temporary stabilization of signal transmission, previous field studies conducted high-altitude release of vaporized f-block metal samarium to undergo spontaneous associative ionization with ambient oxygen. In the process of examining electronic transitions of SmO in the 645 – 670 nm range, an overlap of two rotational structures were found near 665 nm. The present work focuses on spectroscopic studies of separating the overlapping structures and taking rotationally resolved spectra. Rotational constants were derived by spectrum fitting to assist modeling the molecule's spectrum, which could be used to compared with that of the field experiment.

To study the behavior of f electrons in f-block metals, previous studies on actinide metal compound thorium oxyfluoride were conducted. Spectra were found to be not resolvable at high resolution, which was speculated to be due to high density of electronic states. To obtain rotationally resolvable spectra, spectroscopic studies on thorium oxyfluoride were conducted. Resulting spectra were simulated by contoured fit, and rotational constants were estimated.

Spectroscopic Studies of two f-Block Metal Compound

By

Jiarui Yan

Michael Heaven

Adviser

A thesis submitted to the Faculty of Emory College of Arts and Sciences
of Emory University in partial fulfillment
of the requirements of the degree of
Bachelor of Science with Honors

Chemistry

2023

Acknowledgements

I would like to express my sincere gratitude to my advisor, Dr. Michael Heaven, for his invaluable guidance and exhaustive feedback throughout the process of writing this thesis. His expertise and encouragement have been instrumental in shaping my research and helping me to refine my ideas. I would also like to extend my thanks to Arianna Rodriguez, a PhD student on the project, for patiently explaining theoretical concepts and offering valuable insights that have greatly enhanced my understanding of the subject matter. Additionally, I would like to thank all of my colleagues in the lab for their support over the past year and a half.

Table of Contents

Chapter 1: Spectroscopic Study on Lanthanide Compound SmO

Chapter 2: Spectroscopic Study on Actinide Compound OThF

Introduction

When electromagnetic wave signal is transmitted through the ionosphere, it gets fluctuated and scintillated because of the turbulence in the layer. This is because molecules are constantly being hit by the sunlight, including ultraviolets capable of ionizing them. Free electrons are created in this process, and thus creating a natural variation in electron density. As described in previous studies by Shuman et al., this variation can be mitigated by increasing local density of electrons.[1] To achieve this, it was proposed to artificially release chemical species that can produce electrons by undergoing spontaneous associative ionization with the constituents in the atmosphere. A plausible method for creating an electron cloud is to employ an ionization reaction of type $M + O \rightarrow MO^+ + e^-$.[1,2] This requires that the bond dissociation energy of the molecular orbital (MO) is greater than the ionization energy (IE). It was estimated that f-block metal samarium is one of the metals that meets the unusual condition.[2]

Sounding rocket experiments were conducted by launching small amounts of vaporized samarium into the atmosphere to react with ambient oxygen under the exposure of sunlight, creating metal oxide space clouds.[1,3,4] Resulting optical emission signals were recorded. Modeling the field experiment data indicated the production of SmO^+ was lower than estimation based on exothermicity by -0.3eV of the associative ionization.[3-5] Remeasurements of thermodynamics of the reaction were conducted, yielding the reaction is endothermic by 0.048eV, which partially accounts for the low yield of cation species.[5-7]

Early spectroscopic studies were conducted with flame emission techniques to record band spectra of SmO.[8] The resolution was too low for assisting band assignment. Laser-induced fluorescence (LIF) spectra with pulsed laser excitation were done by Hannigan in region of 571 – 654 nm range with vibronic resolution.[9] Bujin et al. recorded isotopically and rotationally resolved spectra, and emission spectra were recorded.[10] Spectroscopic data was assigned to 12 low-lying states of SmO, and electronic map was created.

To experimentally characterize the electronic states of this molecule, electronic transitions of SmO in the 645 – 670 nm range have been examined using laser excitation and dispersed fluorescence techniques.[11] Seven band systems were investigated at the level of rotational resolution, and the spectral range studied was directly related to the field experiment. After deriving the molecular constants for the electronic states, modeling and simulation of the SmO spectrum can be conducted, which can then be used to compared with the field experiment spectrum.

In the process of studying molecular bands, two overlapped bands were found near 15032cm^{-1} (665 nm). The wavelength interval between the most intense peaks was found to be around 0.2 nm. To further study the corresponding electronic states and investigate the bands at rotational resolution, we attempted to separate the structures by conducting LIF spectroscopy and examining dispersed laser induced fluorescence spectra. PGOPHER, a program used for fitting rotational, vibrational, and electronic spectra, was used to conduct line-center fitting of rotationally resolved LIF spectra, and rotational constants were derived.[13]

Experimental

The experimental setup for LIF of SmO is shown in figure 1. A Nd:YAG laser (Quanta-Ray, DCR1A, 10mJ/pulse at 1064nm) was focused onto a samarium rod (American Elements) to produce vaporized samarium. The rod was placed in an ablation block, and was constantly rotated and translated by motors in order to avoid pitting and improve consistency of metal vapor production. Gas pulses were produced by a pulse valve (Parker Hannifin General Valve Series 9) with a pulse duration of 280μs and repetition frequency of 10Hz. The gas mixture was 0.1% of N_2O in He carrier gas, and the backing pressure was 120 psi. The samarium vapor was entrained in the gas mixture, and samarium oxide was produced. The vapor mixture cloud was then supersonically expanded through a 3mm diameter hole from the ablation block into a chamber. The chamber was evacuated by a roots blower (Leybold, RUVAC WSU 251) and a rotary vane pump (Leybold TRIVAC D65B).

To take LIF spectra, the vapor mixture expansion was excited by a tunable dye laser (Lambda-Physik, FL 3002e), where the dye was excited by a 308nm wavelength XeCl excimer (Lambda-Physik, Compex Pro 201), with a frequency of 10Hz. DCM was used in the dye laser, which possesses a range of 615nm to 680nm and emission peak at 643nm. Fluorescence from the expansion was focused by a lens perpendicular to the dye laser and was recorded by a PMT. A long pass filter was used to shield the PMT from scattered light. The PMT signal was sent to an oscilloscope (Tektronix TDS 2014) and a boxcar integrator (Stanford Research System, SRS 250). Signal decay curves were recorded directly from the oscilloscope. To record LIF spectra, the dye laser swept the target region by 0.003nm each increment with 30 averages. Voltage readings from the boxcar were digitized by a National Instruments Data Acquisition Device (NI DAQ), and then recorded as LIF spectra after averaging. To take DLIF spectra, the most intense rotational feature of the vibronic transition was excited. The fluorescence was then sent through the focusing lens into a 0.64 m monochromator equipped with a 1200 grooves/mm diffraction grating. The monochromator was then scanned through the region from 550nm to 800nm.

To calibrate the dye laser's wavelength, a part of the dye laser was reflected into an iodine vapor cell, and iodine spectra were recorded by a PMT (Hamamatsu R966 photomultiplier). The iodine spectra were taken simultaneously as the LIF scan ran and were compared with PGOPHER iodine spectra data to calibrate wavelength. To calibrate the monochromator, an argon calibration lamp was used, and the yielded emission peaks were compared with literature data.

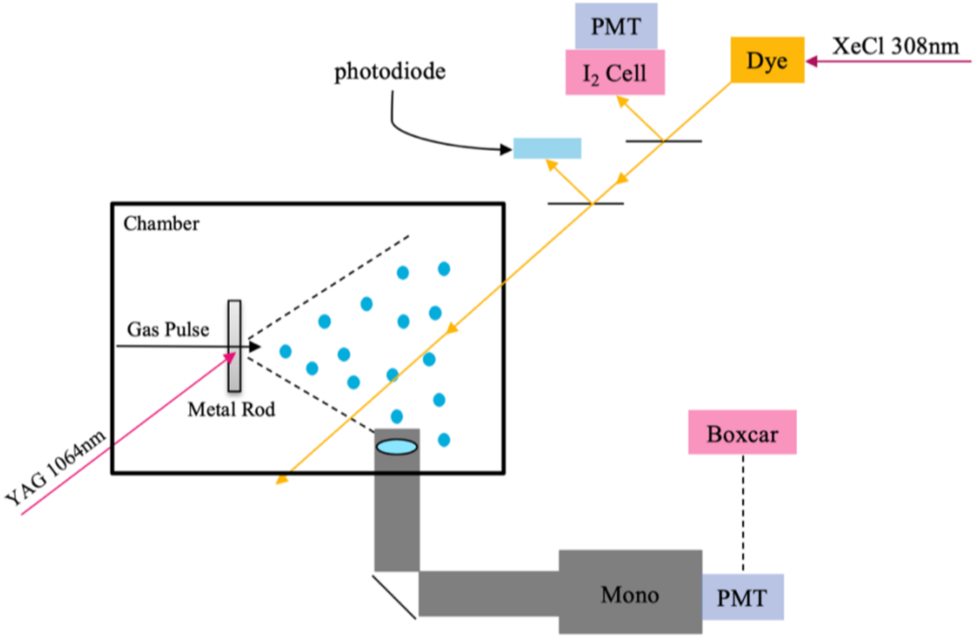

Figure 1. Apparatus used to take LIF and DLIF spectra for samarium oxide. Dye laser goes horizontally into the chamber perpendicular to the expansion and the wall of the chamber. The laser encounters two beam splitters, and the reflected beams excite the iodine cell and trigger the photodiode. After the expansion being excited and fluoresce emission, the light goes vertically through a focusing lens (blue ellipse) and is then sent through the monochromator to the PMT.

Results and Analysis

Survey spectra were recorded around 665 nm (15071.6 – 14970.1 cm^{-1}). As an overlapping of multiple features was present in the same scan, DLIF scans were taken by scanning the monochromator within the range of 550 – 800 nm (12500cm^{-1} to 18181.8cm^{-1}) while the dye laser was set to excitation peaks at 15016cm^{-1} or 15032cm^{-1}. Each spectrum exhibited multiple emissions, indicating the energy of lower electronic states.

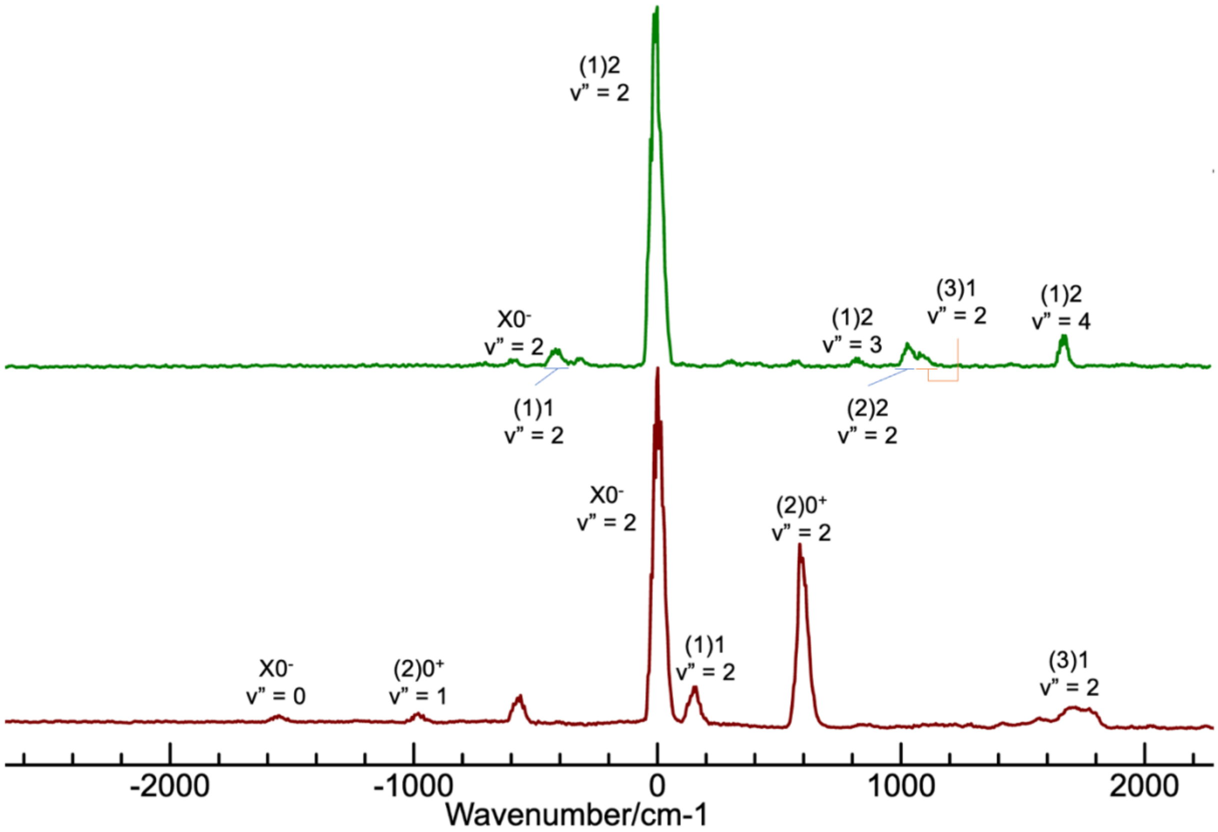

Figure 2. Calibrated DLIF spectra obtained by excitation at 15016cm-1 (green trace) or 15032cm-1 (red trace). The horizontal scale in this figure is the difference between the emission feature and the excitation energy. One emission band in the 15032cm^{-1} spectrum was left unassigned. Emission peaks were assigned and the gap between peaks were compared with literature energy gap by Bujin et al.[10]

LIF scan yielded a rotationally resolved structure with monochromator set to the most intense emission peak at 696nm. A feature fit was conducted by implementing the PGOPHER software package alongside the spectrum to estimate the molecular constants.

In trying to assign the electronic energy level of the 15016cm^{-1} transition, LIF scans were taken by scanning the dye laser with monochromator sitting on the emissions at 13908cm^{-1} (719nm) or 13280cm^{-1}(753nm). The peak at 15003cm^{-1} was not completely suppressed for the former transition, while the latter still yielded an overlapping structure (figure 3). Thus, molecular constants were unable to be determined by spectrum fitting.

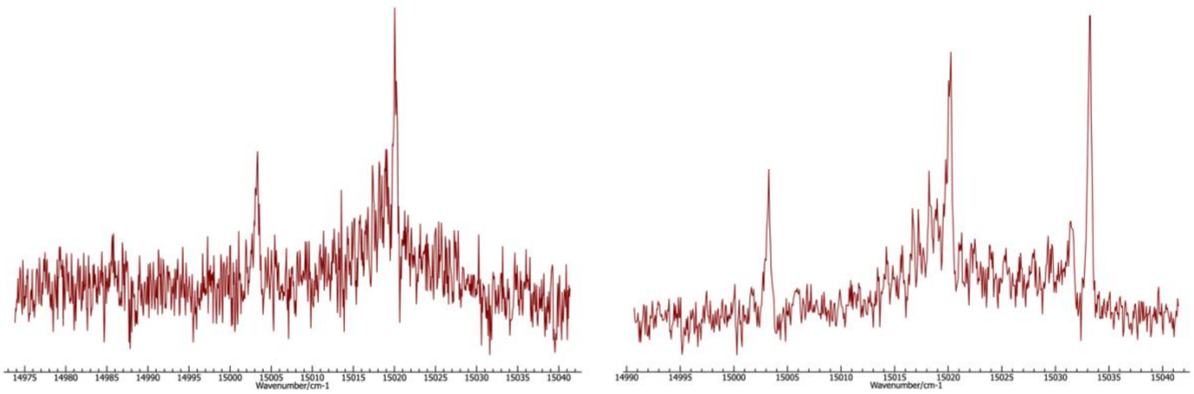

Figure 3. LIF spectra with monochromator set to 13908cm^{-1} (left) and 13280cm^{-1} (right). For the left scan, the peak at 15003cm^{-1} was not suppressed. For the right scan, because of the overlap of two structures, rotational structure cannot be assigned.

Discussion

The band at 15032cm^{-1} was assigned to the 0 – 2 band of the {16.67}1– X0⁻ transition, supported by the molecular constants yielded by fitting rotational structure. By setting temperature to 9K and band origin at 15032cm^{-1}, PGOPHER was implemented to conduct a line-center fitting with some of the resolved branched assigned as shown in figure 5.

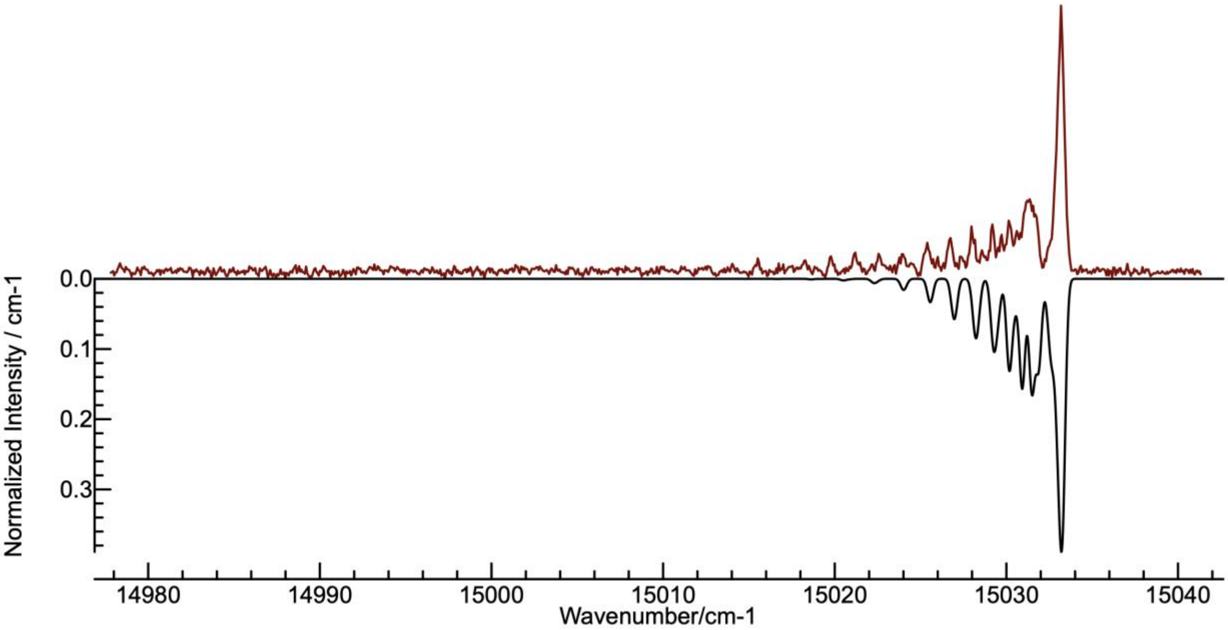

Figure 5. Rotationally resolved LIF spectrum of the {16.67}1– X0⁻ 0 – 2 band. Rotational structures to the left are completely suppressed. The downward-going trace is fitted spectrum by PGOPHER. Rotational temperature used in this model was 9K.

Rotational constants were allowed to float during the fitting process to achieve lower error, and value for constants were shown in table 1. With a reasonably large decrease in the rotational constant, this indicates that the excited state is a charge-transfer state, where one electron from oxygen is transferred back to samarium. For the {17.02}1– (1)2 0 – 2 transition, with failing to separate the rotational structures, spectrum fitting could not be conducted. Thus, molecular constant was unable to be assigned.

Table 1. Molecular constants for SmO by spectrum fitting.

	B” (cm^{-1})	**q” (cm^{-1})**	**B’(cm^{-1})**	**q’(cm^{-1})**
{16.67}1	0.3507	x	0.2622	0.017

Summary

The investigation of electronic transitions in SmO at approximately 665 nm was conducted through excitation and dispersed fluorescence techniques. To minimize spectral congestion, jet-expansion cooling was implemented. Dispersed fluorescence spectra's emission peaks were assigned referencing the literature values by Bujin et al. and attempts to separate the rotational structures were done by scanning the LIFs with the monochromator sent to emission peaks[10]. The rotational constant of the {16.67}1 excited state was derived through a line-centered fitting. This value can aid in the modeling of the molecule and facilitate the simulation of its spectrum for comparison with the results obtained from the field experiment. For the {17.02}1 excited states, as LIF scans with monochromator implemented failed to suppress the features, rotational constant was not able to be determined.

Introduction

Lanthanides tend to have more compacted 4f orbitals compared to the 5f orbitals in actinides. Their partially filled 4f orbitals are not involved in bonding but possess properties similar to those of atomic electrons without contributing to the bonding. To study the behavior of these f electrons, we moved on to the actinide group. Compared to lanthanides' 4f electrons, 5f orbitals in actinides are more extended, and thus may be more involved in bonding[13].

Spectroscopic studies on polyatomic actinides uranium dioxide (UO_2) and its cation were conducted previously in our lab[14,15]. With a ground state rotational constant of approximately $0.16cm^{-1}$, it was expected that electronic spectra could be obtained with rotational resolution. However, the observed spectra for the of the vibronic bands examined could not be resolved at high resolution. It was speculated that this spectral congestion was due to a high density of electronic states. UO_2 was also not the best starting point in terms of electronic permutation complexity. Atomic Uranium has six unpaired valence electrons, bonding with two oxygen atoms makes the UO_2 ground state $O^{2-}U^{4+}(5f7s)O^{2-}$. This leads to a increased electronic complexity with permutation of two electrons among 5f, 6d, and 7s orbitals[16].

To experimentally characterize low-lying states of a model actinide compound, the electronic spectroscopy of OThF was examined. Atomic thorium has four valence electrons, with two residing in 7s orbital and two residing in 6d orbitals. For OThF, as bonding with oxygen takes two electrons and bonding with fluoride takes one electron, there is one unpaired electron in the metal centered 7s orbital. This reduces the electron permutation complexity. It was expected to observe intense transition from 7s to 7p near UV range. OThF has been observed by Lau et al., and the ionization energy (IE) derived was 5.9eV[17]. There is almost no other information for OThF and $OThF^+$ in the literature. Preliminary theoretical calculations were done by using Molpro, a system of ab initio program for molecular electronic calculations, using density function theory (DFT) (B3LYP) and coupled cluster CCSD(T) methods[18]. It was found that both OThF and $OThF^+$ are bent, with bonding angles of 112° and 114°. Rotational constants for OThF were calculated to be 3.84GHz, 5.13GHz, and 15.26GHz, respectively. With reasonably large rotational constants, rotational resolution of spectra for OThF will be feasible. To conduct experimental studies on this molecule, LIF, DLIF, and mass-spectrometry resonance-enhanced multiphoton ionization (REMPI) were implemented.

Experimental

The experimental set-up for of OThF was similar to that used for SmO but was conducted in a different chamber. A thorium rod was mounted in an ablation block and was vaporized by a focused Nd/YAG laser with 1064nm pulses in 10Hz. The rod was constantly rotated and translated to yield avoid pitting. The metal vapor was then entrained into a gas pulse with a mixture of 0.4% O_2 and 0.4% SF_6 in He carrier gas to produce OThF by a pulse valve (Parker-Hannifin series 9). The pulse has a duration of 180μs with 10Hz frequency, and a backing pressure of 100psi.

To take LIF spectra, the expansion was released into a vacuum chamber from an orifice and was excited by the tunable dye laser which was excited by the wavelength XeCl excimer. The fluorescence was detected by a PMT (Photonis XP20200), and was then sent to an oscilloscope (LeCroy WaveSurfer 24Xs). To record the spectra, the dye laser was moved by 0.005nm each increment and was averaged 40 times and digitized by the oscilloscope. To take DLIF spectra, the dye laser was set to the most intense excition peak of the transition, and a monochromator was scanned from 350nm to 650nm.

To setup a resonance-enhanced two photon ionization (RE2PI) scan for OThF, the experiment was carried out in another chamber. Time-of-flight mass spectrometry was used, and the spectra were recorded with mass-resolved ion detection. Molecules with different mass will be shown as discrete peaks on the oscilloscope. In addition to the XeCl laser used in LIF, the other excitation laser was a Continuum ND6000 dye laser driven by a Powerlite 8000Nd/YAG laser. The two dye lasers were aligned such that the same part of the expansion was hit simultaneously by the two dye lasers. The ions were then deflected into an ion detector by a positively charged plate, and signal readings from the detector were then digitized and recorded by the oscilloscope with 30 averages. The dye lasers' wavelengths were calibrated by a Bristol Instruments model 821 wavemeter.

Results and Analysis

Guided by preliminary theoretical calculations, survey spectra detected by means of RE2PI time-of-flight mass spectrometry were taken through the region from 410nm to 460nm, yielding absorptions at 22442cm^{-1} (445.6nm) and at 22936cm^{-1} (436nm). To study their emission spectra, DLIF scans were taken by setting the dye laser to both transitions (sequentially), as shown in figure 6. Each of these traces were shown to possess one molecular emission band. For the 22936cm^{-1} excitation DLIF spectrum, the emission at origin was verified to be pure laser scattering.

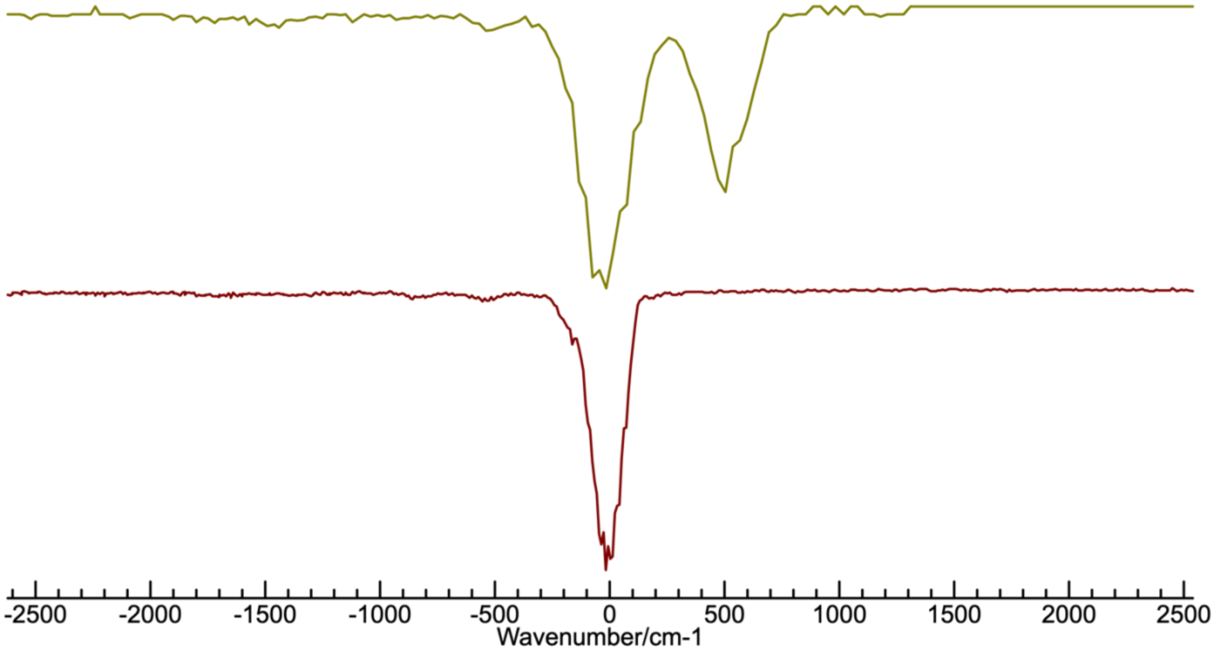

Figure 6. DLIF spectra for excitation at 22442cm^{-1} (upper trace) and 22936cm^{-1} (lower trace). The horizontal scale in this figure is the difference between the emission feature and the excitation energy. The energy gap between the two emissions corresponds to the energy difference between two fluorine vibrational energy levels.

In trying to obtain a more resolved spectrum, an LIF scan the with monochromator set to the most intense peak of emission spectra (445.7 nm) yielded a band at 22442cm^{-1}. A band contour-fit was conducted by PGOPHER as shown in figure 7. Ground state's molecular constants for the 22442 cm^{-1} were obtained from Molpro calculations using DFT (B3LYP) and CCSD(T) methods. A small-core pseudo-potential basis set for Th (ECP60MWB-ANO) and augmented triple-zeta basis sets for O and F (avtz) were used as basis set in the calculation. Calculated ground states rotational constants were used for band fitting.

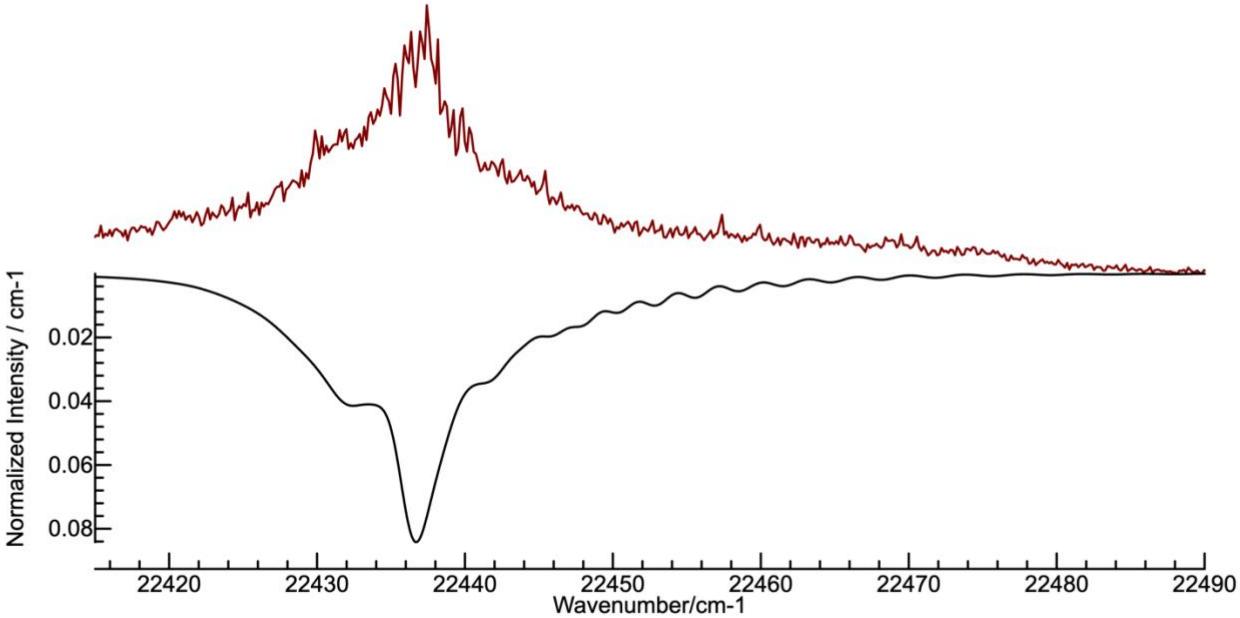

Figure 7. LIF spectrum of 22442cm^{-1} band. Downward-going trace was generated by spectrum fitting using PGOPHER. Rotational temperature was set to 50K, and the bandwidth was set to 2cm^{-1} for this model.

Survey scan identified another OThF transitional band around 28645cm^{-1}. Resulting LIF yielded spectrum that could not be resolved at high resolution. To study the emission spectrum of that band, DLIF scan was conducted, and resulting spectrum is shown in figure 8. We speculate a broad emission is an evidence of increased electronic state density, as electrons relaxed back to a range of states.

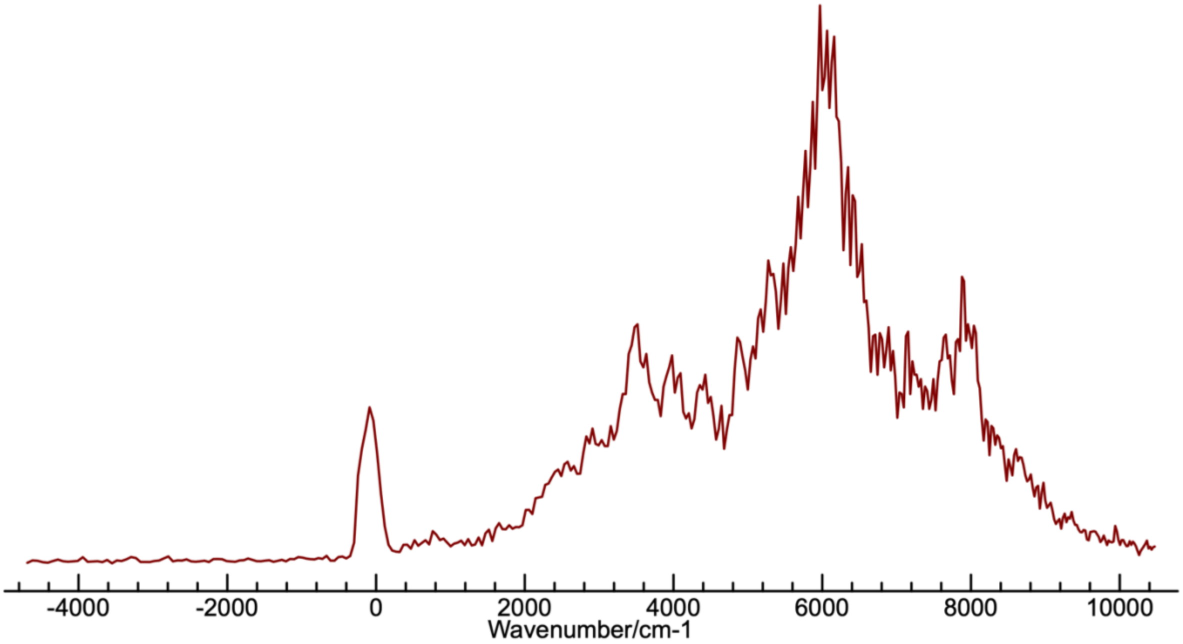

Figure 8. DLIF scan for 28645cm^{-1}. The horizontal scale in this figure is the difference between the emission feature and the excitation energy. A broad distribution of emission features near 6000cm^{-1} indicates there is intense mixing with background states.

Discussion

The ground state's rotational constants for the 22442 cm^{-1} were obtained from Molpro calculations, and the excited state's rotational constants were obtained by contoured fitting. Band origin was set to 22438cm^{-1}. Estimated rotational constants are shown in table 2.

Table 2. Molecular Constants for OThF by spectrum fitting.

	A (cm^{-1})	**B(cm^{-1})**	**C(cm^{-1})**
Ground State	0.541	0.174	0.132
Excited State	0.63	0.147	0.142

To interpret the changes in the rotational constants, with rotational constant A increased, this indicates that the bond angle of the molecule increased on electronic excitation. With rotational constants B and C approaching each other, this indicates that the molecule at the excited states tends more to be a symmetric top, where two moments of inertia possess the same value. A rotationally resolved transitional band is shown in figure 9, juxtaposed with the experimental spectrum. Bandwidth was set to 0.3cm^{-1} which is approximately the linewidth of the dye laser. The deviation between the experimental spectrum and the contoured fit indicates that the structure cannot be resolved at high resolution (0.3 cm^{-1}). It was speculated to be due to a high density of electronic states at this region.

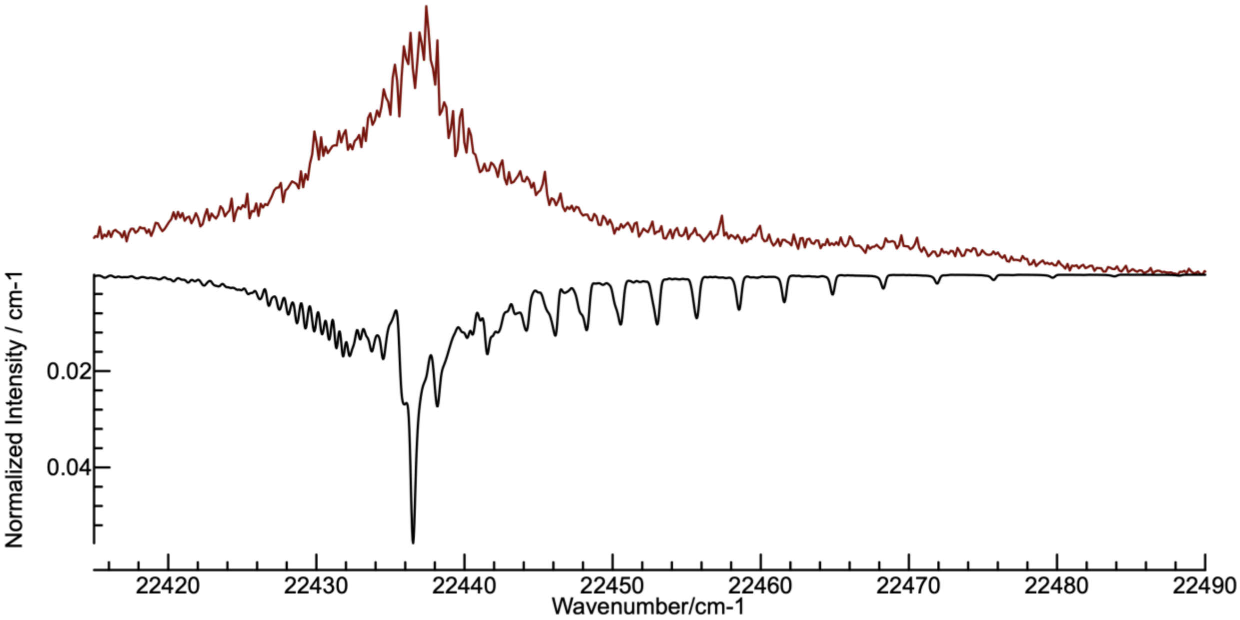

Figure 9. Spectrum fit by setting the temperature to 50K and gaussian was set to 0.3cm^{-1}. This deviates from the experimental spectrum as shown in red trace.

Summary

Electronic transitions of OThF have been examined near 445 nm, 436 nm, and 349 nm using laser excitation and dispersed fluorescence techniques. Electronic structure calculations were performed for the ground state, and rotational constants were derived. Contour-fitting was conducted for the 445 nm transitional band, and the excited state’s rotational constants were determined. For the 349 nm transitional band, the emission spectra yielded intense spectral congestion, suggesting a higher density of states. For future directions, experimental spectroscopic studies are to be conducted on other bands predicted by theoretical calculations, especially states with lower energies to seek for rotationally resolved structure.

Reference

1. Shuman, N. S.; Hunton, D. E.; Viggiano, A. A. Ambient and Modified Atmospheric Ion Chemistry: From Top To Bottom. *Chemical Reviews* **2015**, *115* (10), 4542–4570.

2. Ard, S. G.; Shuman, N. S.; Martinez, O.; Brumbach, M. T.; Viggiano, A. A. Kinetics of Chemi-Ionization Reactions of Lanthanide Metals (Nd, SM) from 150 to 450 K. *The Journal of Chemical Physics* **2015**, *143* (20), 204303.

3. Holmes, J. M.; Dressler, R. A.; Pedersen, T. R.; Caton, R. G.; Miller, D. A Combined Spectroscopic and Plasma Chemical Kinetic Analysis of Ionospheric Samarium Releases. *Radio Science* **2017**, *52* (5), 521–538.

4. Bernhardt, P. A.; Siefring, C. L.; Briczinski, S. J.; Viggiano, A.; Caton, R. G.; Pedersen, T. R.; Holmes, J. M.; Ard, S.; Shuman, N.; Groves, K. M. A Physics-Based Model for the Ionization of Samarium by the MOSC Chemical Releases in the Upper Atmosphere. *Radio Science* **2017**, *52* (5), 559–577.

5. Cox, R. M.; Kim, J. S.; Armentrout, P. B.; Bartlett, J.; VanGundy, R. A.; Heaven, M. C.; Ard, S. G.; Melko, J. J.; Shuman, N. S.; Viggiano, A. A. Evaluation of the Exothermicity of the Chemi-Ionization Reaction Sm + O → SmO+ + e-. *The Journal of Chemical Physics* **2015**, *142* (13), 134307.

6. Armentrout, P. B.; Cox, R. M.; Sweeny, B. C.; Ard, S. G.; Shuman, N. S.; Viggiano, A. A. Lanthanides as Catalysts: Guided Ion Beam and Theoretical Studies of Sm+ + COS. *The Journal of Physical Chemistry A* **2018**, *122* (3), 737–749.

7. Lachowicz, A.; Perez, E. H.; Shuman, N. S.; Ard, S. G.; Viggiano, A. A.; Armentrout, P. B.; Goings, J. J.; Sharma, P.; Li, X.; Johnson, M. A. Determination of the SmO+ Bond Energy by Threshold Photodissociation of the Cryogenically Cooled Ion. *The Journal of Chemical Physics* **2021**, *155* (17), 174303.

8. Piccardi, G. Band Spectra of the Oxides of Praseodymium, Neodymium, and Samarium. *Nature* **1929**, *124* (3129), 618–618.

9. Hannigan, M. C. A Laser Induced Fluorescence Study of SmO. *Journal of Molecular Spectroscopy* **1983**, *99* (1), 235–238.

10. Bujin, G.; Linton, C. Examination of Rotational Structure, Doubling, and Perturbations in 12 Low Lying Electronic States of Samarium Monoxide. *Journal of Molecular Spectroscopy* **1991**, *147* (1), 120–141.

11. Schmitz, J. R.; Le, A. T.; Steimle, T. C.; Rodriguez, A.; Heaven, M. C. Electronic Spectroscopy of SMO in the 645 to 670 Nm Range. *The Journal of Physical Chemistry A* **2022**, *126* (40), 7210–7220.

12. Neidig, M. L.; Clark, D. L.; Martin, R. L. Covalency in F-Element Complexes. *Coordination Chemistry Reviews* **2013**, *257* (2), 394–406.

13. Western, C. M. PGOPHER: A Program for Simulating Rotational, Vibrational and Electronic Spectra. *Journal of Quantitative Spectroscopy and Radiative Transfer* **2017**, *186*, 221–242.

14. Merritt, J. M.; Han, J.; Heaven, M. C. Spectroscopy of the UO2+ Cation and the Delayed Ionization of UO_2. *The Journal of Chemical Physics* **2008**, *128* (8), 084304.

15. Han, J.; Goncharov, V.; Kaledin, L. A.; Komissarov, A. V.; Heaven, M. C. Electronic Spectroscopy and Ionization Potential of UO_2 in the Gas Phase. *The Journal of Chemical Physics* **2004**, *120* (11), 5155–5163.

16. Gagliardi, L.; Heaven, M. C.; Krogh, J. W.; Roos, B. O. The Electronic Spectrum of the UO_2 Molecule. *Journal of the American Chemical Society* **2004**, *127* (1), 86–91.

17. Lau, K. H.; Brittain, R. D.; Hildenbrand, D. L. High Temperature Thermodynamic Studies of Some Gaseous Thorium Fluorides. *The Journal of Chemical Physics* **1989**, *90* (2), 1158–1164.

18. Werner, H.-J.; Knowles, P. J.; Knizia, G.; Manby, F. R.; Schütz, M. Molpro: A General-Purpose Quantum Chemistry Program Package. *Wiley Interdisciplinary Reviews: Computational Molecular Science* **2011**, *2* (2), 242–253.